

New developments of HEMSim: a computational treatment for aluminized highly energetic materials applied to rock blasting

Original

New developments of HEMSim: a computational treatment for aluminized highly energetic materials applied to rock blasting / Caridi, Y., Selesovsky, J., Cucuzzella, A., Vicini, F., Jirman, S., Berrone, S., Pachman, J.. - In: FIREPHYSICHEM. - ISSN 2667-1344. - (2026). [10.1016/j.fpc.2026.03.008]

Availability:

This version is available at: 11583/3009547 since: 2026-04-02T20:19:09Z

Publisher:

Elsevier

Published

DOI:10.1016/j.fpc.2026.03.008

Terms of use:

This article is made available under terms and conditions as specified in the corresponding bibliographic description in the repository

Publisher copyright

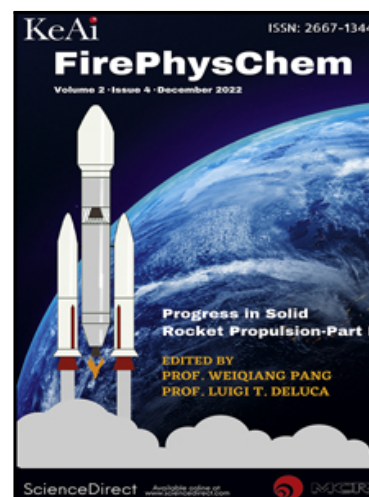
(Article begins on next page)

Journal Pre-proof

New developments of HEMSim: a computational treatment for aluminized highly energetic materials applied to rock blasting

Yuri Caridi, Jakub Selesovsky, Andrea Cucuzzella, Fabio Vicini, Stepan Jirman, Stefano Berrone, Jiri Pachman

PII: S2667-1344(26)00036-2
DOI: <https://doi.org/10.1016/j.fpc.2026.03.008>
Reference: FPC 291



To appear in: *FirePhysChem*

Received date: 5 September 2025
Revised date: 15 March 2026
Accepted date: 15 March 2026

Please cite this article as: Yuri Caridi, Jakub Selesovsky, Andrea Cucuzzella, Fabio Vicini, Stepan Jirman, Stefano Berrone, Jiri Pachman, New developments of HEMSim: a computational treatment for aluminized highly energetic materials applied to rock blasting, *FirePhysChem* (2026), doi: <https://doi.org/10.1016/j.fpc.2026.03.008>

This is a PDF of an article that has undergone enhancements after acceptance, such as the addition of a cover page and metadata, and formatting for readability. This version will undergo additional copyediting, typesetting and review before it is published in its final form. As such, this version is no longer the Accepted Manuscript, but it is not yet the definitive Version of Record; we are providing this early version to give early visibility of the article. Please note that Elsevier's sharing policy for the Published Journal Article applies to this version, see: <https://www.elsevier.com/about/policies-and-standards/sharing#4-published-journal-article>. Please also note that, during the production process, errors may be discovered which could affect the content, and all legal disclaimers that apply to the journal pertain.

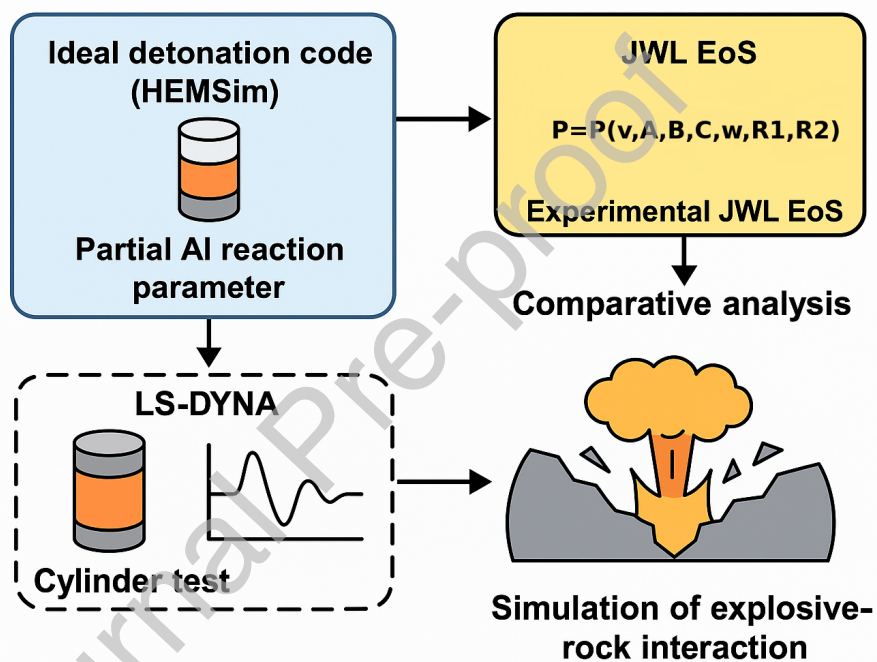
© 2026 Xi'an Modern Chemistry Research Institute. Publishing services by Elsevier B.V. on behalf of KeAi Communications Co. Ltd.

This is an open access article under the CC BY-NC-ND license (<http://creativecommons.org/licenses/by-nc-nd/4.0/>)

Graphical Abstract

New developments of HEMSim: a computational treatment for aluminized highly energetic materials applied to rock blasting

Yuri Caridi^a, Jakub Selesovsky^b,
Andrea Cucuzzella^a, Fabio Vicini^a, Stepan Jirman^b,
Stefano Berrone^b, Jiri Pachman^b



Highlights

New developments of HEMSim: a computational treatment for aluminized highly energetic materials applied to rock blasting

Yuri Caridi^a, Jakub Selesovsky^b,
Andrea Cucuzzella^a, Fabio Vicini^a, Stepan Jirman^b,
Stefano Berrone^b, Jiri Pachman^b

- Using an ideal detonation code (HEMSim) to describe non-ideal explosives.
- Partial Al reaction is used as a parameter to align predictions with experiments.
- Resulting theoretical JWL EoS are compared to the experimental ones.
- LS-DYNA is used to simulate the rock-explosive interaction.

New developments of HEMSim: a computational treatment for aluminized highly energetic materials applied to rock blasting

Yuri Caridi^a, Jakub Selesovsky^b,
Andrea Cucuzzella^a, Fabio Vicini^a, Stepan Jirman^b,
Stefano Berrone^b, Jiri Pachman^b

Politecnico di Torino, Dipartimento di Scienze Matematiche "Giuseppe Luigi Lagrange", Corso Duca Degli Abruzzi 24, Torino, 10129, Italy

University of Pardubice, Faculty of Chemical Technology, Institute of Energetic Materials, Studentska 573, Pardubice, 53210, Czech Republic

Abstract

The purpose of this study is to assess the feasibility of using the ideal detonation code HEMSim to calculate detonation parameters of non-ideal explosives, including aluminized formulations, for subsequent use in hydrodynamic simulations. HEMSim is based on the Chapman-Jouguet (CJ) theory and is not inherently designed to model non-ideal explosives or the delayed energy release associated with aluminum reactions. This limitation complicates the prediction of detonation parameters and Jones-Wilkins-Lee (JWL) equation of state (EoS) parameters required by many blast simulation tools. To address this issue, the HEMSim model was adapted to incorporate a user-defined degree of aluminum reaction completion during detonation, enabling partial aluminum reactivity to be considered. Detonation parameters and JWL EoS parameters were calculated for emulsion explosives containing 0-20% aluminum powder. A series of cylinder tests was conducted to obtain experimental data, from which JWL parameters were derived. These parameters, along with those calculated numerically, were implemented in LS-DYNA hydrodynamic simulations, and simulated cylinder wall velocities were compared with experimental results for validation. The approach was further demonstrated by simulating explosive-rock interaction in a granite specimen. The modified HEMSim approach provides detonation and JWL

parameters that yield good agreement between simulated and experimentally measured cylinder wall velocities. The inclusion of aluminum significantly influences detonation behavior and results in increased damage to rock in numerical simulations. The proposed methodology enables practical prediction of detonation parameters for non-ideal and aluminized explosives using an ideal detonation code. This approach is suitable for hydrodynamic simulations requiring simple JWL inputs and supports the design of more efficient, predictable, and cost-effective blasting operations, particularly when aluminum-containing explosives are employed.

Keywords: Explosive, JWL, Thermochemical Code, Cylinder test, Simulation

1. Introduction

Effective use of explosives in mineral extraction requires a thorough understanding of both the material being fragmented and the properties of the explosive used. Over the past few decades, traditional experimental methods have increasingly been supplemented or replaced by numerical simulations, providing more detailed insights into the rock fracture process. The action of an explosive on its confinement consists of an initial shock-loading phase, followed by the expansion of detonation products [1]. The relative contribution of these two phases depends not only on the type and condition of the rock but also on the characteristics of the explosive itself.

To successfully model the effect of an explosive on surrounding rock, it is essential to describe the expansion of the detonation products numerically. This is typically done using an equation of state (EoS), which defines the thermodynamic behavior of detonation products during adiabatic expansion from the Chapman-Jouguet (CJ) state [2]. Equations of state vary in complexity, ranging from simple empirical models to more advanced, physically based formulations. In hydrodynamic modeling, the selected EoS must strike a balance between computational efficiency and physical accuracy, and must be compatible with the simulation software. One widely used equation, due to its simplicity and integration in many hydrocodes, is the Jones–Wilkins–Lee (JWL) EoS. Originally developed by Lee [3], building on the work of Jones and Miller [4] and Wilkins [5], the JWL EoS defines pressure P as a function of relative volume V :

$$P = A \left(1 - \frac{\omega}{R_1 V} \right) \exp(-R_1 V) + B \left(1 - \frac{\omega}{R_2 V} \right) \exp(-R_2 V) + \frac{\omega E_0}{V}. \quad (1)$$

The JWL equation requires knowledge of six constants (A , B , R_1 , R_2 , ω , and E_0) specific to the explosive being modeled. These parameters may be found in the literature for well-known formulations [6], calculated using thermochemical codes such as Cheetah [7], Carte [8, 9, 10], SIAME [11, 12], TDS [13], EXPLO5 [14, 15], or HEMSim [16], or experimentally derived from cylinder expansion tests [17, 18, 19, 20, 21, 22].

The cylinder test involves detonating an explosive charge inside a copper tube and measuring the velocity of the expanding cylinder wall. The primary goal of this test is to derive EoS parameters from the observed wall motion. This method was originally developed at Lawrence Livermore National Laboratory (LLNL) for ideal, or nearly ideal, military explosives. Commercial explosives, such as the ones based on ammonium nitrate, exhibit significant non-ideal behavior characterized by diameter-dependent detonation velocity, large critical diameters, highly curved detonation fronts, long reaction zones, and strong confinement effect, especially for smaller charge diameters.

These complexities are further amplified when metal powders, such as aluminum, are added to the formulation. Aluminum is commonly included in commercial explosives to increase energy output, but its behavior complicates modeling due to its only partial reaction during detonation. The presence of a thin oxide layer on aluminum particles often delays or prevents reaction within the detonation driving zone (DDZ). However, depending on the explosive formulation and aluminum content, partial reaction may occur [23]. Accurately simulating such behavior requires specialized modeling strategies that are not available in commercial codes or even in many proprietary codes.

In this work, the new ideal detonation code HEMSim (Highly Energetic Materials Simulator) [16, 24] is used to model the highly non-ideal behavior of aluminum-containing emulsion explosives. To address the known limitations inherent in using an ideal detonation framework, a concept of partial aluminum reactivity was applied. Outputs including the Chapman–Jouguet (CJ) state and the fitted Jones–Wilkins–Lee (JWL) EoS parameters are obtained and used in hydrocode simulations. By comparing the numerically predicted cylinder wall velocities with experimental measurements, the effective fraction of reactive aluminum necessary to reproduce the experimentally

observed behavior can be quantified. This value should not be interpreted as the actual amount of aluminum that reacts in DDZ, but rather as a modeling parameter used to approximate the observed detonation performance.

2. HEMSim Software

Ammonium nitrate-based explosives are inherently non-ideal due to their sensitivity to confinement, diameter-dependent detonation velocity, and other factors that affect their detonation behavior. When aluminum powder is added to these explosives, the resulting aluminized compositions become even more non-ideal. Predicting detonation parameters for such systems is particularly challenging due to the complex reaction kinetics and incomplete metal combustion. Since a robust and generally accepted non-ideal detonation code capable of accurately modeling these types of explosives is not available, we adopted a simplified approach using the ideal detonation code HEMSim [16]. This code is still under development and is not yet intended for modeling highly non-ideal explosives; its use in this context is exploratory and aimed at assessing its applicability beyond its original scope by applying the assumption of partial chemical equilibrium.

HEMSim is a computational code designed to simulate detonations based on Chapman-Jouguet (CJ) theory, **which** assumes a steady-state, one-dimensional detonation wave governed by the conservation laws of mass, momentum, and energy. The CJ condition defines the state of the reaction products at the sonic point, **where** the detonation velocity reaches its minimum value that still allows for a self-sustained detonation.

The code determines the composition of the detonation products by assuming chemical equilibrium. This is achieved by mathematically modeling the equilibrium state of a multi-phase system through minimization of the Helmholtz free energy, subject to the constraint of mass conservation. Since the system is closed, the elemental quantities, b , remain constant. However, the species quantities, n , can vary as chemical reactions take place.

Nine gaseous product species (H_2 , N_2 , O_2 , CO , NO , H_2O , CO_2 , NH_3 , and CH_4) and ten condensed-phase species (two allotropic forms of carbon (C_{graphite} and C_{diamond}), inert and reactive aluminum, silicon, and sodium oxides in both solid (s) and liquid (l) forms) are considered in the equilibrium calculations. Reaction products of aluminum oxidation, particularly alumina (Al_2O_3), are also accounted for in both solid and liquid states, along with any remaining unreacted aluminum (Al). HEMSim enforces both thermal

and mechanical equilibrium between the gas and condensed phases, ensuring that all phases share a common temperature and pressure at equilibrium.

To describe the thermodynamic properties of materials, HEMSim utilizes specific EoS for each phase. For the gaseous phase, it applies the EXP-6 EoS, which is derived from the Buckingham potential and provides an accurate representation of intermolecular interactions at high pressures and temperatures. For condensed phases, the extended Murnaghan EoS is used, accounting for material compressibility as well as temperature-dependent effects.

To account for the presence of aluminum in the detonation process, it is assumed that a fixed fraction of the total aluminum content reacts to form aluminum oxide (Al_2O_3), which may appear in either liquid or solid form. The remaining aluminum is treated as inert and may also exist in either liquid or solid state.

All other detonation products are assumed to remain in chemical equilibrium during the isentropic expansion phase, up to a fixed temperature T_f . **Once the product mixture reaches T_f (2100 K), its composition is frozen.**

The pressure–volume (P – V) data obtained from this equilibrium-based isentropic expansion model are then used to determine the coefficients A , B , R_1 , R_2 , ω , and E_0 of the Jones–Wilkins–Lee (JWL) equation of state. This approach enables characterization of the explosive behavior within the ideal detonation framework while incorporating the distinct thermodynamic contributions of both reactive and inert aluminum components.

A central component of the chemical equilibrium model is the formula matrix M **in Tab. 2**, where rows correspond to the chemical species in the detonation products and columns to the constituent elements of the original formulation.

To account for the incomplete reaction of aluminum within the reaction zone, a user-defined parameter Rf is introduced, representing the fraction of aluminum moles that react relative to the total aluminum present. This parameter, which is a numerical construct, is typically inferred from experimental data. The equilibrium calculation must therefore allow for constrained reaction extent. Specifically, the stoichiometry of aluminum oxide formation, which requires two aluminum atoms per Al_2O_3 molecule, must be enforced along with the linear mass balance constraints defined by M :

$$n_{\text{Al}_2\text{O}_3(\text{s})} + n_{\text{Al}_2\text{O}_3(\text{l})} = \frac{Rf}{2} b_{\text{Al}}. \quad (2)$$

| | H | C | N | O | Al | Si | Na |
|------------------------------------|---|---|---|---|----|----|----|
| H ₂ (g) | 2 | 0 | 0 | 0 | 0 | 0 | 0 |
| N ₂ (g) | 0 | 0 | 2 | 0 | 0 | 0 | 0 |
| O ₂ (g) | 0 | 0 | 0 | 2 | 0 | 0 | 0 |
| CO(g) | 0 | 1 | 0 | 1 | 0 | 0 | 0 |
| NO(g) | 0 | 0 | 1 | 1 | 0 | 0 | 0 |
| H ₂ O(g) | 2 | 0 | 0 | 1 | 0 | 0 | 0 |
| CO ₂ (g) | 0 | 1 | 0 | 2 | 0 | 0 | 0 |
| NH ₃ (g) | 3 | 0 | 1 | 0 | 0 | 0 | 0 |
| CH ₄ (g) | 4 | 1 | 0 | 0 | 0 | 0 | 0 |
| C _{(s),diam} | 0 | 1 | 0 | 0 | 0 | 0 | 0 |
| C _{(s),grap} | 0 | 1 | 0 | 0 | 0 | 0 | 0 |
| Al _(s) | 0 | 0 | 0 | 0 | 1 | 0 | 0 |
| Al _(l) | 0 | 0 | 0 | 0 | 1 | 0 | 0 |
| Al ₂ O ₃ (s) | 0 | 0 | 0 | 3 | 2 | 0 | 0 |
| Al ₂ O ₃ (l) | 0 | 0 | 0 | 3 | 2 | 0 | 0 |
| SiO ₂ (s) | 0 | 0 | 0 | 2 | 0 | 1 | 0 |
| Na ₂ O(s) | 0 | 0 | 0 | 1 | 0 | 0 | 2 |

Table 1: Formula matrix for the product species considered in HEMSim.

where $n_{\text{Al}_2\text{O}_3}$ indicates the molar concentration of aluminum oxide in solid or liquid phase and b_{Al} indicates the number of aluminum atoms in the reactant.

The motivation for introducing Rf in the present work is not to replace experimental fitting, nor to suggest a new fundamental physical parameter, but to address a practical and well-known limitation faced by a large fraction of numerical modellers. In preliminary design studies or parametric simulations, direct experimental calibration of JWL parameters for specific aluminized formulations is generally not possible due to cost, safety, or infrastructure constraints. Unavailability of a commercial non-ideal detonation code leaves users with the simplified ideal detonation software only. In these situations modellers do not have too many options and a simplified approach regarding aluminum reactivity may be the only way to allow them to proceed. We also emphasize that the proposed approach is not intended to be universally transferable to all classes of explosives. The reduction factor should be regarded as formulation- and application-dependent. However, the emulsion explosive used in this study is representative of a broad class of emulsion explosives commonly employed in civil applications, particularly in rock blasting and mining. We therefore believe that the conclusions drawn here are relevant for a substantial range of practical engineering applications, while acknowledging that different explosive types, especially of a military nature, may require different effective parameterization.

3. Materials and methods

Five types of emulsion explosives (one pure and four with Al powder) were tested in duplicate. All compositions represent highly non-ideal explosives. Wall velocities from the cylinder test were measured and used to calculate the JWL equation of state (JWL_{CTEV}). Every set of the JWL parameters was used to simulate the wall motion during the cylinder test using LS-DYNA hydrocode. The JWL parameters were also determined using thermodynamic calculation (HEMSim code, $\text{JWL}_{\text{HEMSim}}$). The detonation properties, including the expansion JWL parameters, were calculated for varying amounts of Al with selected levels of reactivity. The simulated wall velocities were compared to the experimental ones. Finally, LS-DYNA was used to simulate rock-explosive interaction in a small-scale model. The scheme of experimental and simulation procedures is displayed in Figure 1.

The experimental and numerical methodology comprised six sequential stages. First, five emulsion explosive mixtures were prepared with varying aluminum

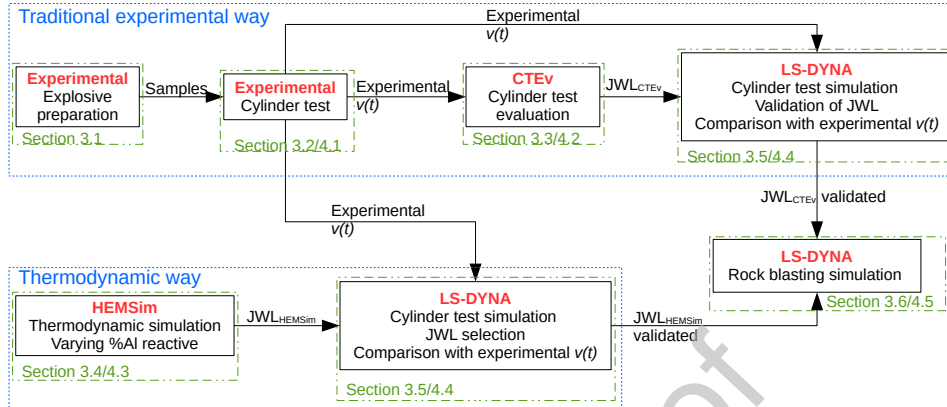


Figure 1: The flowchart of experimental and simulation sections.

content. Second, cylinder tests were conducted to measure detonation performance. Third, the experimental data were evaluated using CTEv software to derive JWL parameters (designated JWL_{CTEv}). Fourth, thermodynamic simulations were performed using HEMSim with varying assumptions regarding aluminum reactivity to obtain theoretical JWL parameters (designated JWL_{HEMSim}). Fifth, hydrodynamic simulations of the cylinder test were conducted using LS-DYNA with both sets of JWL parameters. Finally, the approach was demonstrated through hydrodynamic simulation of explosive-rock interaction in a granite specimen.

In the results and discussion, we compare the simulated velocity profiles with the experimental ones and determine the level of reacted Al providing the best match to the experimental results.

3.1. Explosive preparation

The unsensitized emulsion matrix was prepared by Explosia a.s. semi-plant unit (Czech Republic). The matrix contained 67.77% of ammonium nitrate (AN), 12.50% of sodium nitrate (SN), 11.92% of water, 6.25% of oil, and 1.56% of Lubrizol 2724 by mass. The sensitization and addition of the aluminum (Ecka emulsion grade 150, Non Ferrum Switzerland, Switzerland) were done on-spot before filling the explosive into the cylinders by adding a 3.3% (m/m) of glass micro balloons (GMB) and the appropriate amount of Al powder.

The aluminum concentration is with respect to a sensitized matrix, meaning that in the case of, e.g., 10%, the explosive contained 10% of Al and 90%

Table 2: Composition of the tested explosives (weight percents).

| sample | Al | GMB | AN | SN | water | oil | Lubrizol 2724 |
|--------|----|------|-------|-------|-------|------|---------------|
| A | 0 | 3.30 | 65.53 | 12.09 | 11.53 | 6.04 | 1.51 |
| B | 5 | 3.14 | 62.26 | 11.48 | 10.95 | 5.74 | 1.43 |
| C | 10 | 2.97 | 58.98 | 10.88 | 10.37 | 5.44 | 1.36 |
| D | 15 | 2.81 | 55.70 | 10.27 | 9.80 | 5.14 | 1.28 |
| E | 20 | 2.64 | 52.43 | 9.67 | 9.22 | 4.84 | 1.21 |

of the sensitized matrix by mass. The concentration of GMB, therefore, varied between the compositions based on the amount of Al as shown in Table 2.

3.2. Cylinder test setup

The sample was filled into the oxygen-free copper tube (DHP copper, supplied by OZM Research, Czech Republic). Nominally, 25 and 30 mm were the inner and outer diameters, and 300 mm was the tube length. The exact dimensions of each tube's internal and external diameters were measured with the Mitutoyo caliper, and the wall thickness was measured with the Mitutoyo wall thickness micrometer. Each parameter was measured at 5 positions, the diameter along the pipe length, and the wall thickness at the edges. These precise values were used for evaluation and the simulations. The properties of the tested charges are shown in Table 3.

The velocity of the wall tube was measured using two (samples A and B) or three (samples C, D, and E) PDV sensors (collimators, inclined 5°). Custom built Photonic Doppler Velocimeter manufactured by University of Pardubice (Czech Republic), was used. The detonation velocity was measured using 5 channels of Optimex-64, manufactured by OZM Research (Czech Republic). The measurements were done in duplicate. The scheme of the cylinder test can be seen in Figure 2.

3.3. Cylinder test evaluation

To describe the explosive for JWL calculation, one needs to know its density, detonation velocity, and detonation pressure. Whereas measurement of the density and the detonation velocity is simple, the measurement of detonation pressure is not. Indirect methods [25] can be used; however, their application is difficult for the cases of explosives with a long reaction zone

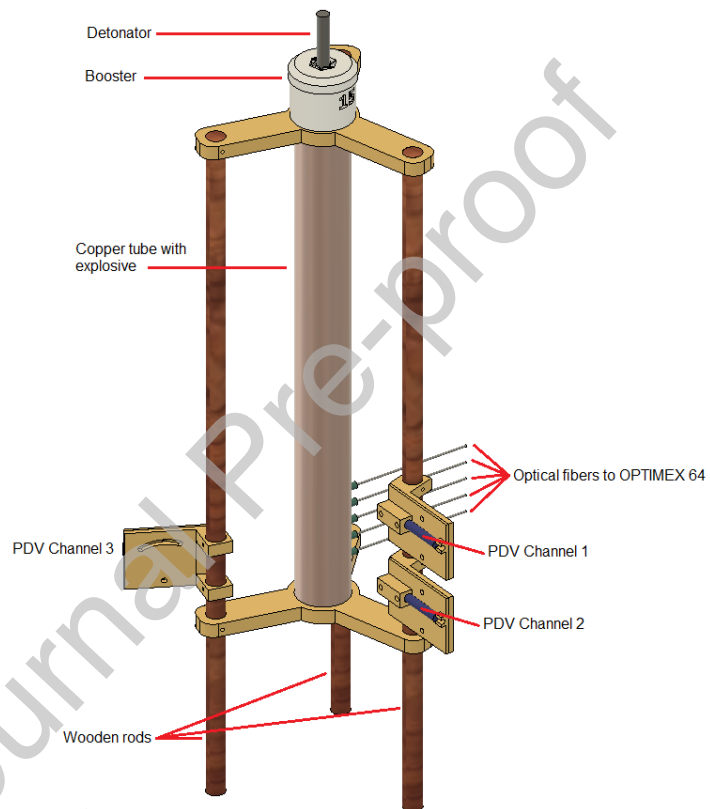


Figure 2: The scheme of the cylinder test.

Table 3: Properties of tested charges.

| Shot | Sample | ρ^1 (g/cm ³) | d^2 (mm) | s^3 (mm) |
|------|--------|-------------------------------|------------|------------|
| 1 | A | 1.00 | 25.35 | 2.49 |
| 2 | A | 1.00 | 25.35 | 2.51 |
| 3 | B | 1.00 | 23.31 | 2.51 |
| 4 | B | 1.00 | 25.30 | 2.49 |
| 5 | C | 1.11 | 25.30 | 2.49 |
| 6 | C | 1.10 | 25.35 | 2.51 |
| 7 | D | 1.13 | 25.35 | 2.59 |
| 8 | D | 1.13 | 25.40 | 2.52 |
| 9 | E | 1.15 | 25.30 | 2.49 |
| 10 | E | 1.16 | 25.35 | 2.54 |

¹density²inner tube diameter³wall thickness

using a standard-sized cylinder test. A detonation pressure was therefore estimated with an alternative approach, based on the density ρ and detonation velocity D . Equation (3), proposed by Cooper [2], was found to be the most appropriate [26]:

$$P_{CJ} = \rho D^2 (1 - 0.7125\rho^{0.04}) \quad (3)$$

Parameters of JWL EoS were calculated according to [21] with two modifications:

- The JWL pressures were optimized for more relative volumes. The original approach optimizes the pressure only for relative volumes equal to $V_r = 2.4, 4.4,$ and 7.0 . We have used a sequence of relative volumes from $V_r = 1.5$ to $V_r = 7.0$, with a step of 0.5 .
- Only two main corrections were applied. First for the wall thinning and second for copper work hardening.

All the cylinder test evaluations were done with CTEv (Cylinder Test Evaluation), an in-house code which calculates JWL EoS from measured wall velocity profiles [26].

3.4. Thermodynamic simulation with HEMSim

HEMSim code was used to compute the CJ parameters (D , P_{CJ}) and JWL constants (A , B , R_1 , R_2 and ω) for each explosive. The fraction of Al reacting directly in a detonation zone (samples B-E) was varied from 0% (aluminum does not react) to 100% (all aluminum reacts) with a 20% step. The energy E_0 was taken for the expansion to an infinite volume.

3.5. Hydrocode modeling of cylinder test

The cylinder tests were simulated with LS-DYNA. The axial symmetry was employed, and the simulations were done in 2D. A uniform Eulerian mesh with a resolution of 5 elements per mm was used. The inner and outer radii of a copper tube were adjusted to the experimental values for each shot. The length of the tube was shortened to 200 mm.

The main charge was characterized by the new JWL (*EOS_JWL keyword) set obtained from experimental data (CTEv) or the results of HEM-Sim (with varying fraction of Al reacting). The beta burn flag was activated in *MAT_HIGH-EXPLOSIVE_BURN keyword to achieve a curved profile of the detonation front. Beta burn needs to be initiated by the booster (PETN based plastic explosive Semtex 1A). The copper tube was characterized by Johnson-Cook constitutive model (*MAT_JOHNSON_COOK) and linear polynomial equation of state (*EOS_LINEAR_POLYNOMIAL). The air was described as an ideal gas (keywords *MAT_NULL and *EOS_LINEAR_POLYNOMIAL). The wall velocity profile was processed using trigonometry to achieve a velocity profile "as seen by probe", enabling direct comparison to experimental data. All the LS-DYNA keywords are explained in the second volume of LS-DYNA keyword manual [27].

3.6. Hydrocode simulation of rock-explosive interaction

A proper modeling of a blasting process requires a reliable description of both the explosive and the rock. Since we do not have any experimental data from rock blasting, we have adopted a small-scale model of a granite rock specimen (fresh rock with uniaxial compressive strength 120 MPa) from [28], S6.

The granite rock specimen has the form of a cylinder with a diameter of 240 mm and a height of 300 mm. A central borehole has a diameter of 17.1 mm and a depth of 206 mm. The borehole has been filled with 15 mm of the explosive. Above the charge is 101 mm of an air deck and 90 mm of sand stemming. The whole model is displayed in Figure 3. The ALE method was

used. The explosive, air, and stemming were modeled as Euler materials, and the rock as Lagrange material. Nominal size of the mesh was 1 mm.

The explosive was modeled with standard burn (keywords `*MAT_HIGH-EXPLOSIVE_BURN`, beta burn flag 0, and `*EOS_JWL`). The air was modeled as an ideal gas (with keywords `*MAT_NULL` and `*EOS_LINEAR_POLYNOMIAL`), and the stemming as a sand (`*MAT_SOIL_AND_FOAM`). The granite rock specimen was modeled with RHT constitutive model (`*MAT_RHT`). All the material constants for air, sand, and granite can be found in [28]. All the LS-DYNA keywords are explained in the second volume of LS-DYNA keyword manual [27].

Three simulations were carried out for three parameter sets of explosives. Sample A, characterized by HEMSim, serves as a baseline. To see the effect of aluminum addition, sample D, characterized by HEMSim (80% of reactive aluminum), was simulated (parameters from Table 8). To see the difference between theoretical (HEMSim) and experimental (CTEv) characterization of the explosive, sample D, characterized by CTEv (parameters in Table 6), was simulated.

This set of simulations can be evaluated only in qualitative manner, due to the lack of experimental data. If the usage of Rf in HEMSim is suitable for the determination of JWL parameters of aluminized emulsion explosives, the damage patterns for theoretical and experimental JWL coefficients of sample D will be similar. In this case, the JWL from HEMSim with using of Rf is suitable for a different application than a cylinder test.

4. Results and discussion

4.1. Cylinder test

The influence of aluminum addition on the experimentally measured cylinder wall velocities can be seen in Figure 4. The terminal velocities, read from the experimental velocity profiles, are presented in Table 4. As expected, the terminal velocities increase with the increasing Al content, whereas the initial velocity jump is not significantly affected.

4.2. Cylinder test evaluation

The velocity profiles shown in Figure 4 were evaluated with CTEv, leading to Figure 5. Each velocity profile was processed separately. Figure 5 shows the reproducibility of JWL parameters calculation from two shots (each with three PDV probes) for sample C (with 10% Al). The individual parameters

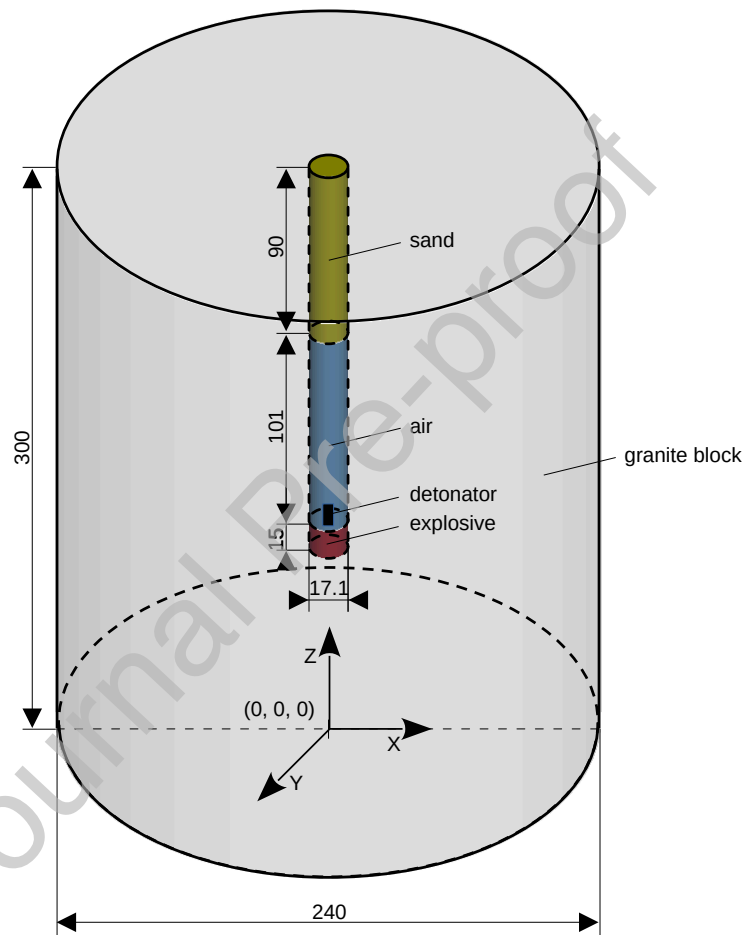


Figure 3: The model used for rock-explosive interaction simulation.

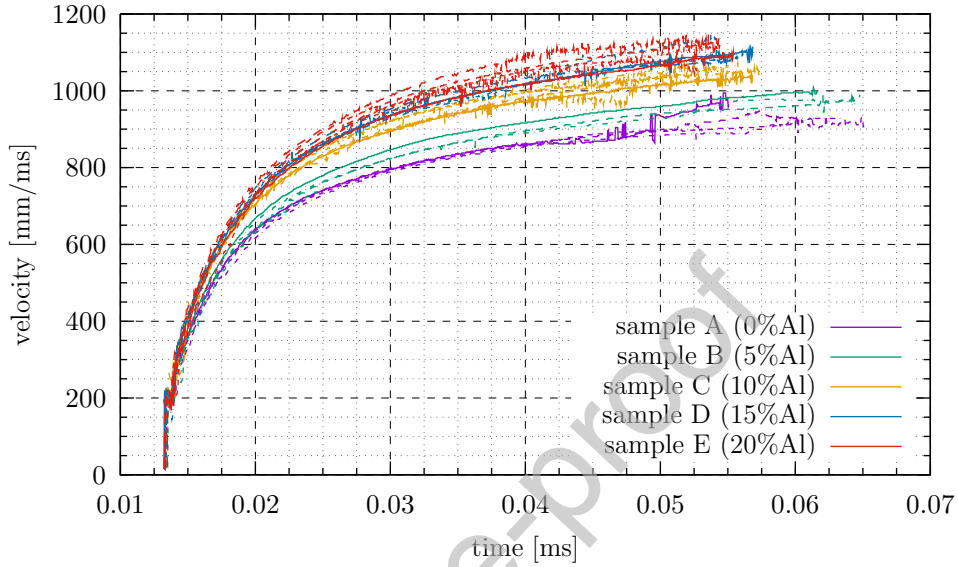


Figure 4: Experimental velocity time histories showing the effect of Al addition. The terminal velocities increase with the increasing Al content.

Table 4: Terminal velocities from cylinder test.

| Sample | Individual terminal velocities (m/s) | | | | | | \bar{v}_t^1 (m/s) | $s_{v_t}^2$ (m/s) |
|-----------|--------------------------------------|------------------|------------------|------|------------------|------------------|---------------------|-------------------|
| A (0%Al) | 860 | 915 | 896 | 897 | N/A ³ | N/A ³ | 892 | 23 |
| B (5%Al) | 996 | N/A ⁴ | 924 | 962 | N/A ³ | N/A ³ | 961 | 36 |
| C (10%Al) | 1033 | 1014 | 1041 | 986 | 1055 | 1050 | 1030 | 26 |
| D (15%Al) | 1099 | N/A ⁴ | N/A ⁴ | 1089 | N/A ⁴ | 1078 | 1088 | 11 |
| E (20%Al) | 1090 | 1072 | 1112 | 1123 | N/A ⁴ | 1124 | 1104 | 23 |

¹mean

²standard deviation

³samples A and B were measured only with two probes per shot

⁴incomplete record

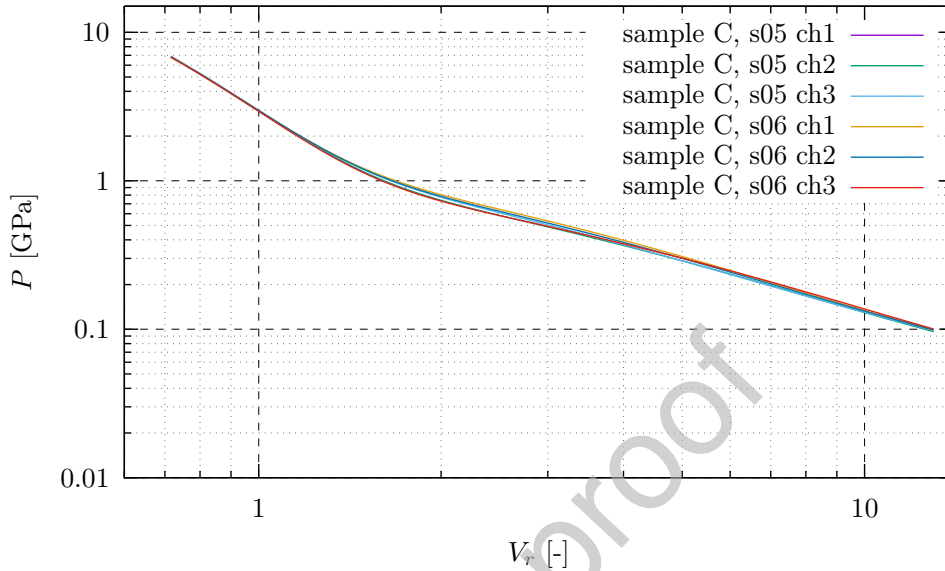


Figure 5: The reproducibility of JWL evaluated with CTEv, sample C, shots 5 and 6 (s05 and s06), three velocity profiles each (ch1, ch2, and ch3).

of JWL EoS can not be compared directly; only a comparison of the whole $P(V_r)$ relationship makes sense. It can be seen that the differences between individual $P(V_r)$ in Figure 5 are only minor.

4.3. HEMSim simulations

Detonation of each composition was simulated with the HEMSim code, with varying amounts of Al, reacting directly in the detonation zone. The effect of increasing reactive Al content can be seen in Figure 6 for sample E (20% Al). The total energy (represented by the area under the $P-V$ curve) grows with the increasing content of reacting Al, as was expected.

4.4. Cylinder test simulations

The last step of the JWL determination is the comparison of the experimental wall velocity profiles with the velocity profiles obtained from a hydrocode with the new JWL.

The comparison of experimental and simulated (JWL from CTEv) wall velocity profiles is demonstrated by Figure 7 for sample C (10% Al). The simulated profiles slightly overestimate velocity; however, the difference does

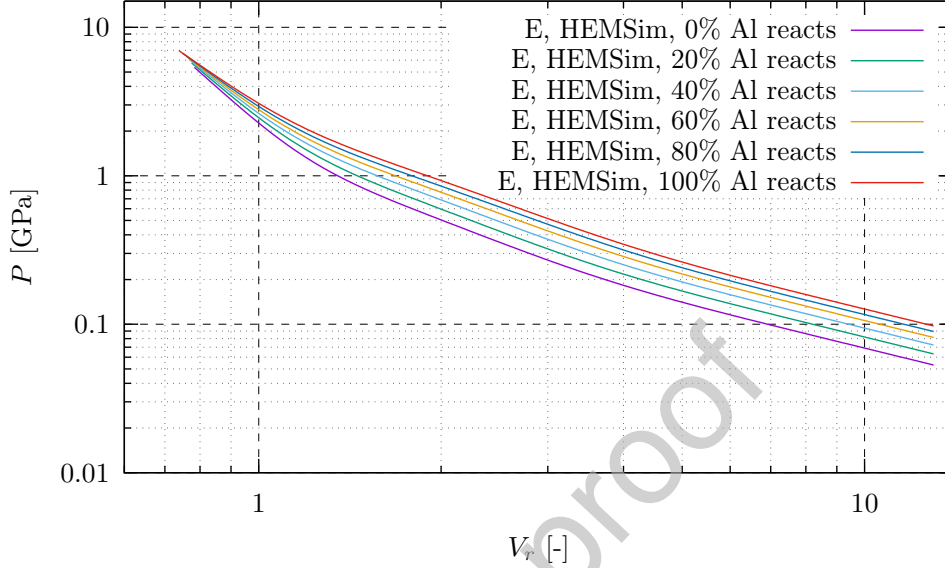


Figure 6: The comparison of JWL (HEMSim) for sample E with varying content of Al reacting in the detonation zone.

not exceed 50 m/s, which corresponds to the difference from individual signals. A similar comparison for other samples can be seen in Figure 8. The differences between experimental and simulated wall velocity profiles do not exceed the experimental scatter for each sample.

Terminal velocities, read from individual simulations, are presented in Table 5. In comparison with Table 4, the mean value for sample A (0% Al) is overestimated, the mean values for the other samples are similar to the corresponding experimental values.

The measured detonation velocity D , CJ pressure (estimated by Equation 3), and JWL coefficients calculated by CTEv are summarized in Table 6. CTEv evaluates every velocity profile itself. However, only one resulting JWL set was selected for each sample. The differences are only minor, as stated previously (Figure 5). Despite the individual parameters of the JWL EoS are not being comparable, parameter E_0 is an exception. It corresponds to the energy liberated at detonation/expansion. Parameter E_0 grows with the increasing Al content, as was expected.

The experimental wall velocity profiles are compared to the ones simulated with detonation velocity, CJ pressure, and JWL coefficients from HEM-

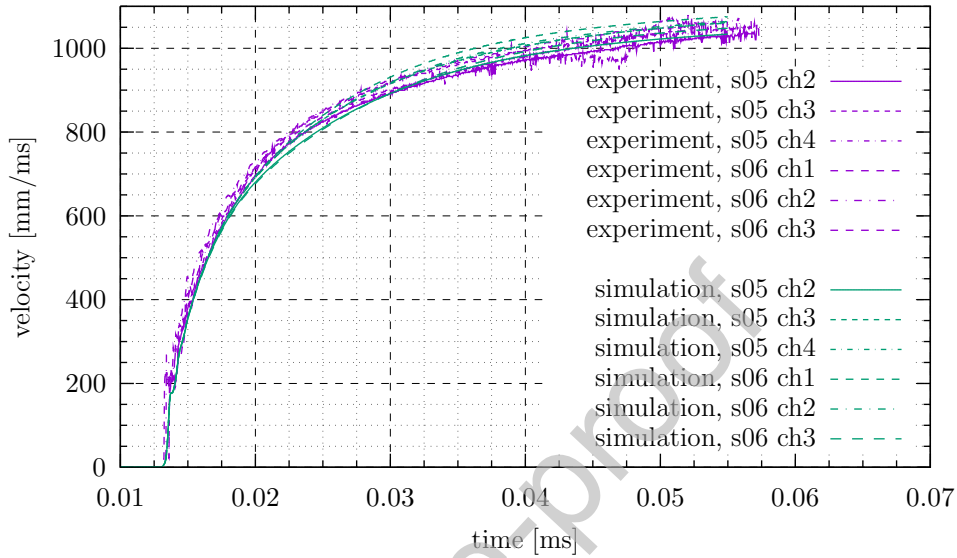


Figure 7: The comparison of experimental and simulated (JWL from CTEv) wall velocities for sample C (10% Al). 'sXX' corresponds to shot number XX, 'chY' corresponds to individual PDV probes.

Table 5: Terminal velocities from cylinder test simulations (JWL parameters from CTEv).

| Sample | Individual terminal velocities (m/s) | | | | | | \bar{v}_t^1 (m/s) | $s_{v_t}^2$ (m/s) |
|-----------|--------------------------------------|------------------|------|------|------------------|------------------|---------------------|-------------------|
| A (0%Al) | 933 | 959 | 944 | 946 | N/A ³ | N/A ³ | 946 | 11 |
| B (5%Al) | 994 | N/A ⁴ | 972 | 989 | N/A ³ | N/A ³ | 985 | 12 |
| C (10%Al) | 1033 | 1061 | 1060 | 1075 | 1064 | 1048 | 1057 | 15 |
| D (15%Al) | 1075 | 1073 | 1080 | 1083 | 1047 | 1097 | 1076 | 16 |
| E (20%Al) | 1076 | 1104 | 1091 | 1119 | 1094 | 1133 | 1103 | 21 |

¹mean

²standard deviation

³samples A and B were measured and simulated only with two probes per shot

⁴JWL was not evaluated, incomplete experimental record

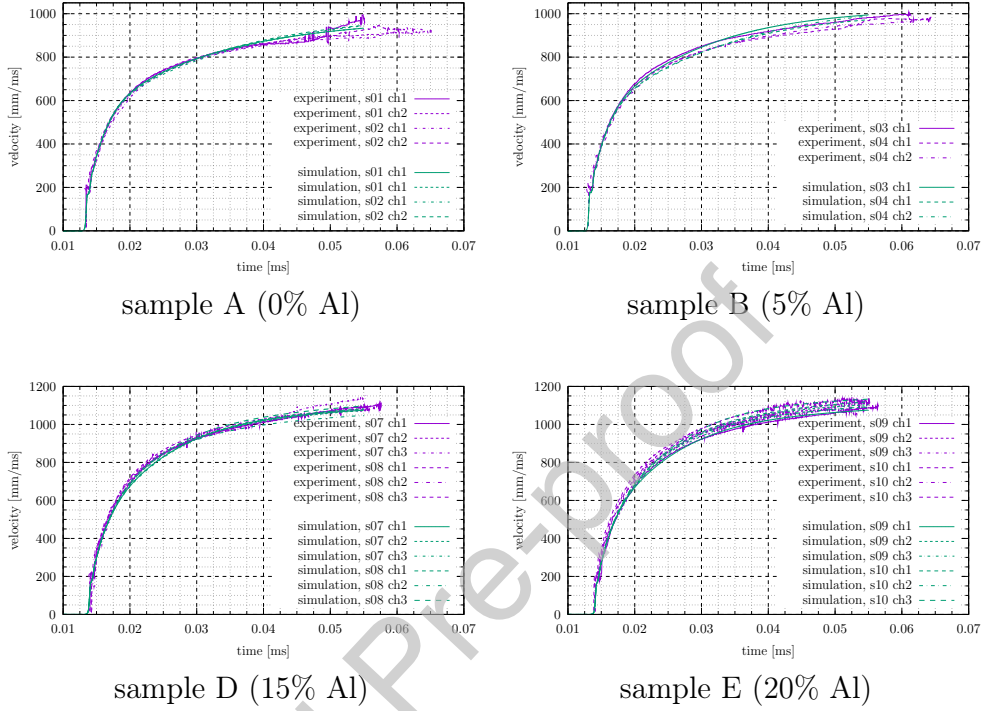


Figure 8: The comparison of experimental and simulated (JWL from CTEv) wall velocities for remaining samples. 'sXX' corresponds to shot number XX, 'chY' corresponds to individual PDV probes.

Table 6: The CJ properties of tested samples, JWL constants from CTEv.

| Sample | D (km/s) | P_{CJ} (GPa) | A (GPa) | B (GPa) | R_1 (-) | R_2 (-) | E_0 (GPa) | ω (-) |
|--------|---------------|-------------------|--------------|--------------|--------------|--------------|----------------|-----------------|
| A | 4.82 | 6.68 | 86.19 | 0.04988 | 3.877 | 0.166 | 3.75 | 0.28 |
| B | 4.90 | 6.90 | 89.74 | 0.10713 | 3.880 | 0.186 | 3.91 | 0.28 |
| C | 4.80 | 7.25 | 104.49 | 0.33358 | 4.052 | 0.367 | 3.95 | 0.28 |
| D | 4.71 | 7.12 | 115.39 | 1.14398 | 4.458 | 1.006 | 4.66 | 0.32 |
| E | 4.67 | 7.13 | 109.79 | 0.66236 | 4.226 | 0.419 | 4.88 | 0.27 |

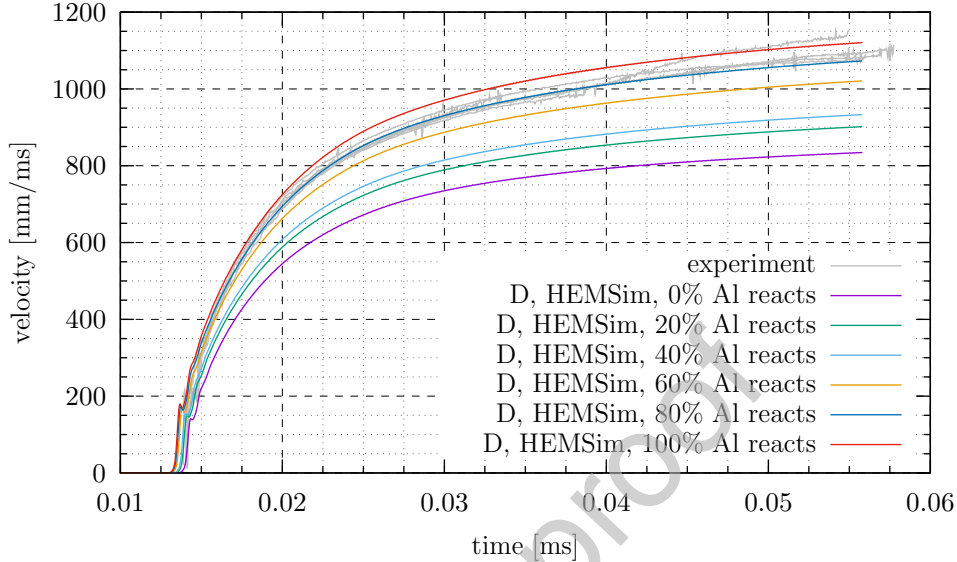


Figure 9: The comparison of experimental and simulated (CJ and JWL from HEMSim) wall velocities for sample D (15% Al). The terminal velocities increase with the increasing Al reactivity.

Sim for sample D (15% Al) in figure 9. The more Al reacts in the CJ state, the more energy is released, thus the terminal wall velocity grows. The profile corresponding to 80% of reacting aluminum best matches the experimental data. The results for sample E are similar; 80% of Al reacting produces the best result. For the samples B and C with smaller total aluminum content, the best correspondence is, however, achieved for 100% of reactive aluminum. The results for the samples A, B, C, and E are plotted in Figure 10.

Read terminal velocities, from simulations with HEMSim explosives parameters, are for all samples presented in Table 7. The value of terminal velocity most corresponding to the mean experimental value (Table 4) are highlighted. These corresponds to the values of Rf 0% (sample A), 100% (samples B and C) and 80% (samples D and E).

The results of HEMSim calculations are summarized in Table 8. The results for 100% (samples B and C) or 80% (samples D and E) of reacting Al are stated, respectively. It is important to say that this result does not mean that 80% (or 100%) of Al reacts in the detonation zone. It can be said only that if one sets the reactivity of Al to 80% (100%) in an ideal detonation code, the resulting simulated wall velocity profile best matches

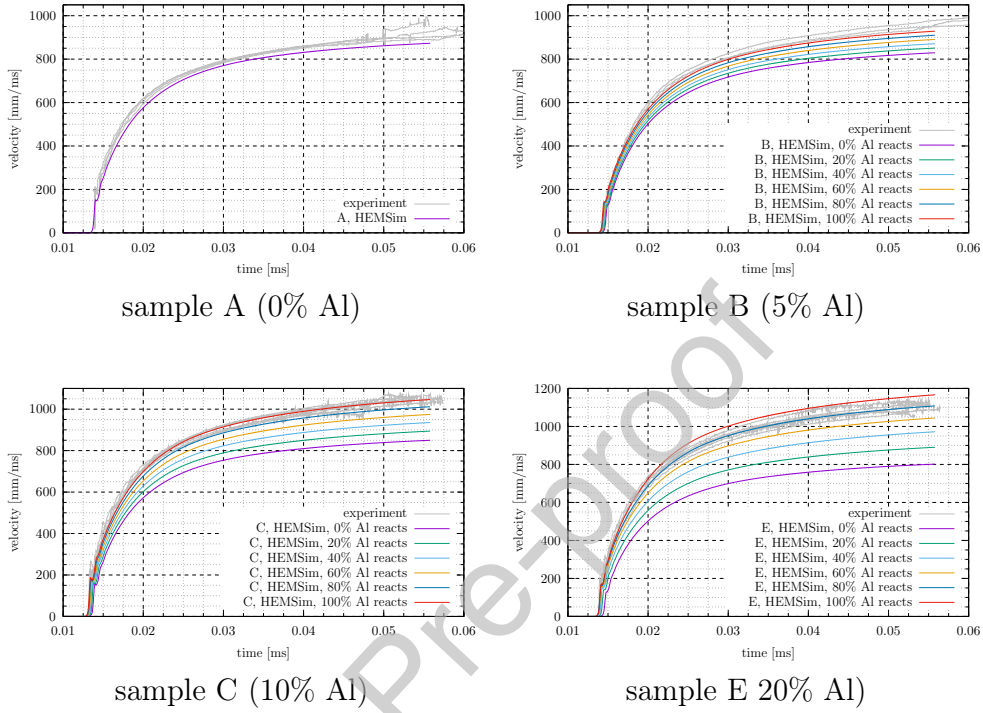


Figure 10: The comparison of experimental and simulated (CJ and JWL from HEMSim) wall velocities for remaining samples. The terminal velocities increase with the increasing Al reactivity.

Table 7: Terminal velocities from cylinder test simulations (CJ and JWL parameters from HEMSim). Values most corresponding to the mean of experimental terminal velocities are in bold.

| Sample/ Rf | Individual terminal velocities (m/s) | | | | | |
|--------------|--------------------------------------|-----|-----|------|-------------|-------------|
| | 0% | 20% | 40% | 60% | 80% | 100% |
| A (0%Al) | 873 | N/A | N/A | N/A | N/A | N/A |
| B (5%Al) | 829 | 851 | 871 | 891 | 910 | 929 |
| C (10%Al) | 850 | 894 | 935 | 974 | 1012 | 1046 |
| D (15%Al) | 834 | 902 | 933 | 1021 | 1073 | 1120 |
| E (20%Al) | 801 | 891 | 972 | 1045 | 1108 | 1166 |

Table 8: The CJ properties and JWL_{HEMSim} constants from HEMSim. 100% of reacting aluminum is assumed for samples B and C, 80% of reacting aluminum is assumed for samples D and E.

| Sample | D (km/s) | P_{CJ} (GPa) | A (GPa) | B (GPa) | R_1 (-) | R_2 (-) | E_0 (GPa) | ω (-) |
|--------|---------------|--------------------------|--------------|--------------|--------------|--------------|----------------|-----------------|
| A | 4.88 | 5.65 | 265.8 | 2.508 | 5.56 | 1.27 | 2.83 | 0.29 |
| B | 4.78 | 5.55 | 257.545 | 2.677 | 5.68 | 1.29 | 3.83 | 0.26 |
| C | 5.05 | 6.74 | 333.091 | 3.143 | 5.72 | 1.23 | 4.96 | 0.23 |
| D | 4.97 | 6.66 | 349.929 | 3.130 | 5.81 | 1.22 | 5.28 | 0.21 |
| E | 4.87 | 6.68 | 339.225 | 3.172 | 5.83 | 1.19 | 5.97 | 0.20 |

the experimental one from the cylinder test.

4.5. Simulation of rock-explosive interaction

Figure 11-13 show cross-sections of the granite cylinder at plane $y = 0$, with rock damage (history variable 4) displayed. Following Li et al. [28], damage values above 0.4 are considered complete failure; therefore, only elements with damage between 0 and 0.4 are shown to illustrate the damage progression.

If one compares the damage pattern produced by emulsion A (without Al, figure 11) and the damage pattern produced by emulsion D (15% Al, figure 12), it is clear that the addition of Al results in larger damage of a tested granite block. This result was expected; this is exactly the reason for the Al addition.

More interesting is the comparison of figures 12 and 13. Both figures correspond to emulsion D with 15% Al. For the first case, the explosive was characterized theoretically with HEMSim (80% Al was assumed to react). For the second case, the explosive was characterized by an experimental cylinder test. The damage patterns are not the same, but they are very similar. The usage of an ideal detonation code with the assumption of partially reacting Al produces similar results as experimental characterization of the explosive.

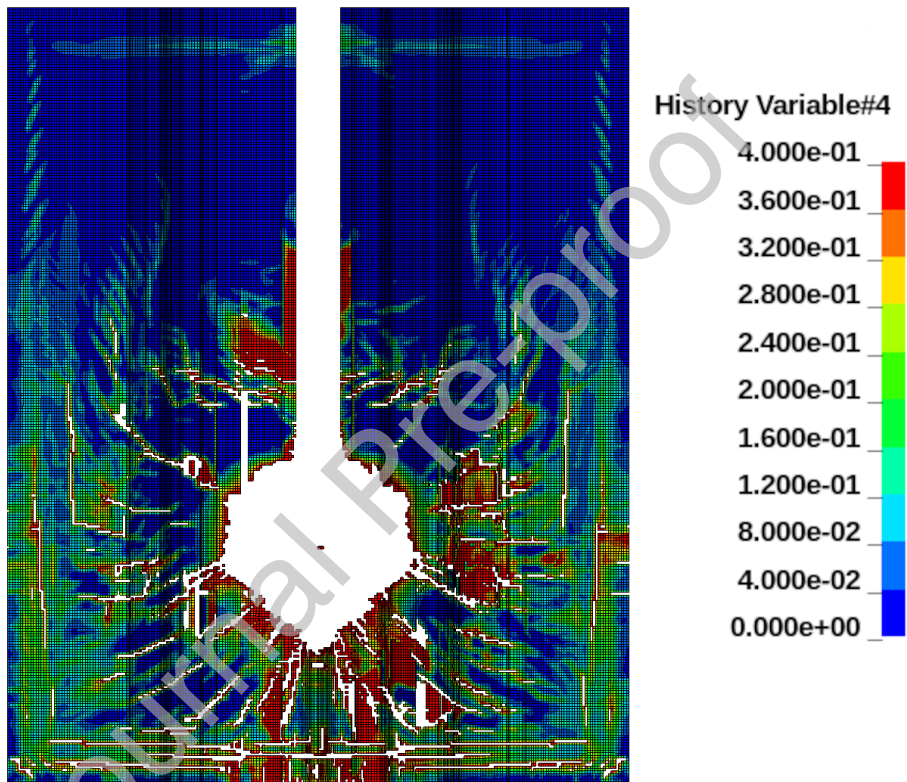


Figure 11: The damage of a granite rock specimen block, cut at $y = 0$, $t = 50 \mu\text{s}$, emulsion A (without Al), characterized with HEMSim. Only elements with damage lower than 0.4 are displayed.

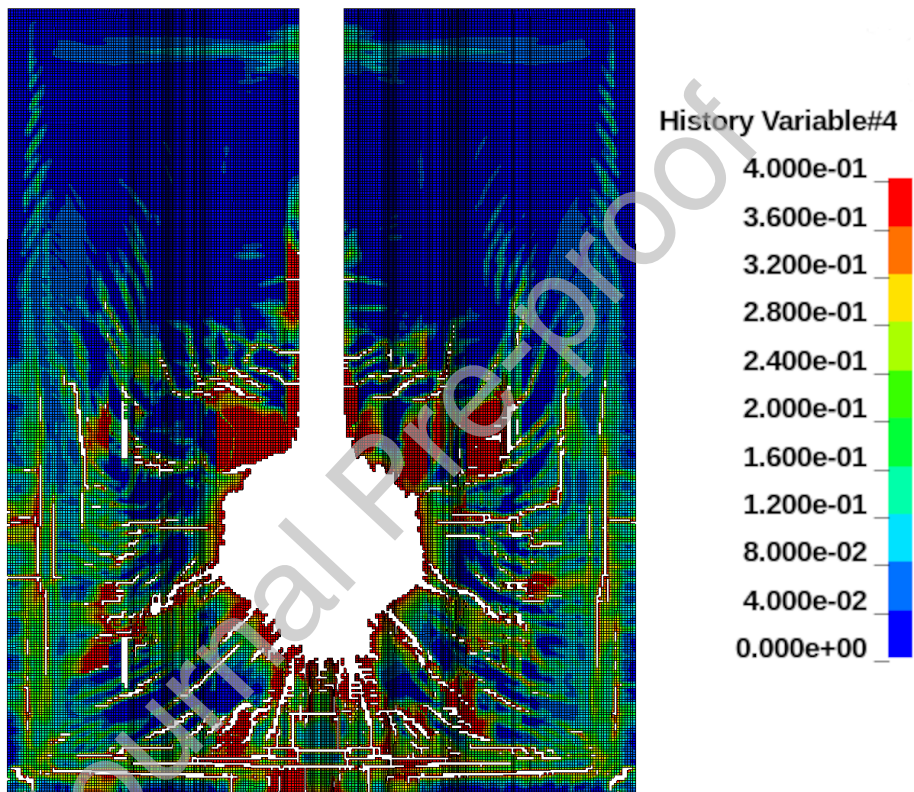


Figure 12: The damage of a granite rock specimen block, cut at $y = 0$, $t = 50 \mu\text{s}$, emulsion D (15% Al), characterized with HEMSim with 80% of reactive aluminum. Only elements with damage lower than 0.4 are displayed.

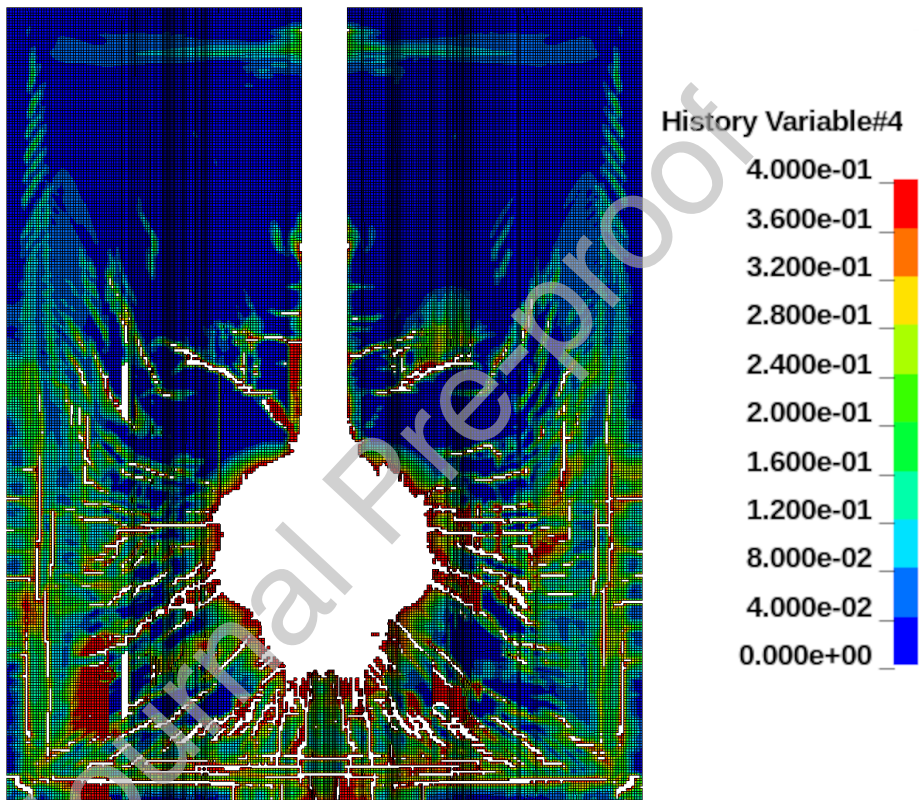


Figure 13: The damage of a granite rock specimen block, cut at $y = 0$, $t = 50 \mu\text{s}$, emulsion D (15% Al), characterized experimentally. Only elements with damage lower than 0.4 are displayed.

5. Conclusion

Effective use of explosives in mineral extraction requires a comprehensive understanding of both the material to be fragmented and the properties of the explosive employed. This study focuses on the characterization of commercial explosives based on ammonium nitrate, which are inherently non-ideal. The addition of aluminum, used to increase energy output in the expansion phase, further enhances this non-ideality, introducing additional complexity to the description of the detonation process. As a result, standard ideal detonation thermodynamic codes based on the Chapman–Jouguet (CJ) theory are inadequate for reliably describing the behavior of such explosives.

To address these challenges, we adapted the HEMSim code, in its current state suitable for modeling ideal detonations, to include the concept of partial aluminum reactivity. We recognize that using an ideal detonation code like HEMSim for modeling non-ideal explosives is inherently limited. However, by introducing an artificial assumption of incomplete aluminum reaction, we create a pragmatic workaround that enables a better match with experimental results. Five types of emulsion explosives containing 0–20% aluminum were characterized experimentally using cylinder tests, derivation of JWL equations of state, and hydrocode simulations for validation. These explosives were also modeled in HEMSim across a range of aluminum reactivity assumptions (0–100%). The best agreement with experimental wall velocities was achieved by assuming 80% reactive aluminum for explosives with 15–20% Al, and full (100%) reactivity for those with 5–10% Al.

To further validate this approach, a small-scale rock–explosive interaction model, adapted from the literature and implemented in LS-DYNA, was used to simulate the detonation of the 15% Al emulsion. The simulations based on both experimental and HEMSim-derived parameters produced comparable rock damage patterns. These results support the idea that partial aluminum reactivity, though a simplification, can serve as an effective tool for characterizing non-ideal explosives within the framework of ideal detonation modeling. At present, no computational code fully capturing the complex physical and chemical processes in the detonation wave of non-ideal explosives is publicly available to the mining community; therefore, such an engineering approximation remains necessary for practical applications.

6. Acknowledgement

Yuri Caridi, Andrea Cucuzzella, Fabio Vicini, and Stefano Berrone are members of Gruppo Nazionale Calcolo Scientifico-Istituto Nazionale di Alta Matematica (GNCS-INdAM).

The authors thanks the INdAM-GNCS Project “Metodi numerici efficienti per problemi accoppiati in sistemi complessi” (CUP E53C24001950001).

This work was partially funded by the University of Pardubice through a grant SGS_2025_003.

7. Declaration of generative AI and AI-assisted technologies in the writing process.

During the preparation of this work, the authors used ChatGPT and Grammarly to improve the readability of the manuscript. After using this tool, the authors reviewed and edited the content as needed and take full responsibility for the content of the published article.

Declaration of interests

The authors declare that they have no known competing financial interests or personal relationships that could have appeared to influence the work reported in this paper.

References

- [1] Lindsay, C.M., Butler, G.C., Rumchik, C.G., Schulze, B., Gustafson, R., Maines, W.R., 2010. Increasing the utility of the copper cylinder expansion test. *Propellants, Explosives, Pyrotechnics* 35, 433–439. doi:10.1002/prop.201000072.
- [2] Cooper, P.W., 1996. *Explosives Engineering*. 1st ed., Wiley-VCH, New York, NY, USA.
- [3] Lee, E.L., Hornig, H.C., Kury, J.W., 1968. Adiabatic expansion of high explosive detonation products. Technical Report UCRL-50422. USA.
- [4] Jones, H., Miller, A.R., 1948. The detonation of solid explosives: the equilibrium conditions in the detonation wave-front and the adiabatic expansion of the products of detonation. *Proceedings of the Royal Society of London A* 194, 480–507. doi:10.1098/rspa.1948.0093.

- [5] Wilkins, M.L., Squier, B., Halperin, B., 1965. Equation of state for detonation products of pbx 9404 and lx04-01. Symposium (International) on Combustion 10, 769–778. doi:10.1016/S0082-0784(65)80220-X.
- [6] Dobratz, 2023. Properties of chemical explosives and explosive simulants. URL: <https://katalog.upce.cz/records/75b4d064-1660-4ffd-8ae5-8f30aededf14>. accessed: Jul. 27, 2023.
- [7] Fried, L.E., Howard, W.M., Souers, P.C., 1998. Cheetah 2.0 User's Manual. Technical Report. LLNL.
- [8] Dubois, V., Pineau, N., 2016. New developments of the carte thermochemical code: A two-phase equation of state for nanocarbons. Journal of Applied Physics 119, 015903. doi:10.1063/1.4938528.
- [9] Desbiens, N., Dubois, V., Matignon, C., Sorin, R., 2011. Improvements of the carte thermochemical code dedicated to the computation of properties of explosives. Journal of Physical Chemistry B 115, 12868–12874. doi:10.1021/jp206890h.
- [10] Dubois, V., Desbiens, N., Auroux, E., 2010. New developments of the carte thermochemical code: Calculation of detonation properties of high explosives. Chemical Physics Letters 494, 306–311. doi:10.1016/j.cplett.2010.05.093.
- [11] Poeuf, S., 2018. Equations of state of detonation products of solid explosives. Ph.D. thesis. Sciences et Ingénierie en Matériaux, Mécanique, Energétique et. URL: <https://tel.archives-ouvertes.fr/tel01955764>.
- [12] Osmont, A., Genetier, M., Baudin, G., 2018. Ability of thermochemical calculation to treat organic peroxides, in: Proceedings of the Conference of the American Physical Society Topical Group on Shock Compression of Condensed Matter, St. Louis, MO, USA. p. 150030. doi:10.1063/1.5044986.
- [13] Gubin, S.A., 2001. A thermochemical code (tds) for thermodynamic calculations of complex chemical systems. URL: <http://www.icders.org/publications.html>.

- [14] Suceska, M., Braithwaite, M., Klapötke, T.M., Stimac, B., 2019. Equation of state of detonation products based on exponential-6 potential model and analytical representation of the excess helmholtz free energy. *Propellants Explosives Pyrotechnics* 44, 564–571. doi:10.1002/prop.201800339.
- [15] Suceska, M., Chan, H.Y.S., Stimac, B., Dobrilovic, M., 2022. Bkw eos: History of modifications and further improvement of accuracy with temperature-dependent covolumes of polar molecules. *Propellants Explosives Pyrotechnics* doi:10.1002/prop.202100278.
- [16] Caridi, Y., Cucuzzella, A., Berrone, S., 2024. HEMSim: a new MATLAB software to simulate the behavior of highly energetic materials upon Chapman-Jouguet hypothesis. *Journal of Energetic Materials* , 1–16doi:10.1080/07370652.2024.2446906.
- [17] Fuchs, B.E., 1995. Picatinny Arsenal cylinder expansion test and a mathematical examination of the expanding cylinder. Technical Report ARAED-TR-95014. ARDEC. URL: <https://apps.dtic.mil/sti/pdfs/ADA300526.pdf>.
- [18] Chaos, M., 2022. Revisiting the kinematics of the cylinder test. *Propellants Explosives Pyrotechnics* 47, e202100349. doi:10.1002/prop.202100349.
- [19] Lan, I.F., Hung, S.C., Chen, C.Y., Niu, Y.M., Shiuan, J.H., 1993. An improved simple method of deducing JWL parameters from cylinder expansion test. *Propellants Explosives Pyrotechnics* 18, 18–24. doi:10.1002/prop.19930180104.
- [20] Sanchidrián, J.A., Castedo, R., López, L.M., Segarra, P., Santos, A.P., 2022. Determination of the JWL constants for ANFO and emulsion explosives from cylinder test data.
- [21] Souers, P.C., Minich, R., 2015. Cylinder test correction for copper work hardening and spall. *Propellants Explosives Pyrotechnics* 40, 238–245. doi:10.1002/prop.201400135.
- [22] Souers, P., Vitello, P., 2015. Detonation Energy Densities from the Cylinder Test. Technical Report LLNL-TR-666420. LLNL. doi:10.2172/1179424.

- [23] Tappan, B.C., Bowden, P.R., Manner, V.W., Son, S.F., Lichthardt, J.P., Francois, E.G., McDonald, D., 2018. Exploring the effects of reactive additives in explosives in search of higher efficiency with various energetic combinations, in: *New Trends in Research of Energetic Materials*, Pardubice.
- [24] Caridi, Y., Cucuzzella, A., Vicini, F., Berrone, S., 2025. A box-bounded non-linear least square minimization algorithm with application to the jwl parameter determination in the isentropic expansion for highly energetic material simulation. *Algorithms* 18. URL: <https://www.mdpi.com/1999-4893/18/6/360>, doi:10.3390/a18060360.
- [25] Pachman, J., Künzel, M., Němec, O., Majzlík, J., 2018. A comparison of methods for detonation pressure measurement. *Shock Waves* 28, 217–225. doi:10.1007/s00193-017-0761-5.
- [26] Selesovsky, J., Pachman, J., Kucera, J., 2022. Cylinder test of emulsion explosives: possibilities of detonation pressure estimation, in: *New Trends in Research of Energetic Materials*, Pardubice.
- [27] ANSYS, 2023. LS-DYNA keyword user's manual, Volume 2, Material models, R14@ad6b3a9c5.
- [28] Li, X., Liu, K., Sha, Y., Yang, J., Hong, Z., 2023. Numerical investigation on blast-induced rock fragmentation with different stemming structures. *Geomech. Geophys. Geo-energ. Geo-resour.* 9. doi:10.1007/s40948-023-00654-9.